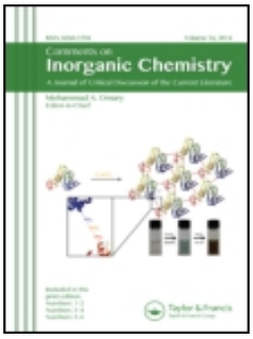

Comments on Inorganic Chemistry
A Journal of Critical Discussion of the Current Literature

ISSN: 0260-3594 (Print) 1548-9574 (Online) Journal homepage: https://www.tandfonline.com/loi/gcic20

# ON THE POSSIBILITY OF SYNTHESIZING $BiMnO_3$ AT AMBIENT PRESSURE USING LOW-TEMPERATURE METHODS

**Inna V. Lisnevskaya, Vera V. Butova, Mikhail I. Perebeinos, Ksenia V. Myagkaya, Andrey O. Letovaltsev, Victor V. Shapovalov, Heba Y. Zahran, Ibrahim S. Yahia & Alexander V. Soldatov**

**To cite this article:** Inna V. Lisnevskaya, Vera V. Butova, Mikhail I. Perebeinos, Ksenia V. Myagkaya, Andrey O. Letovaltsev, Victor V. Shapovalov, Heba Y. Zahran, Ibrahim S. Yahia & Alexander V. Soldatov (2019): ON THE POSSIBILITY OF SYNTHESIZING $BiMnO_3$ AT AMBIENT PRESSURE USING LOW-TEMPERATURE METHODS, Comments on Inorganic Chemistry, DOI: 10.1080/02603594.2019.1643331

**To link to this article:** https://doi.org/10.1080/02603594.2019.1643331

Published online: 05 Aug 2019.

*Comments on Inorganic Chemistry*, 0: 1–17, 2019

ISSN: 0260-3594 print / 1548-9574 online
DOI: https://doi.org/10.1080/02603594.2019.1643331

# ON THE POSSIBILITY OF SYNTHESIZING $BiMnO_3$ AT AMBIENT PRESSURE USING LOW-TEMPERATURE METHODS

Inna V. Lisnevskaya,[1] Vera V. Butova,[2,3] Mikhail I. Perebeinos,[1] Ksenia V. Myagkaya,[1] Andrey O. Letovaltsev,[1] Victor V. Shapovalov,[2] Heba Y. Zahran,[4,5] Ibrahim S. Yahia,[4,5] and Alexander V. Soldatov[2]

[1]Faculty of Chemistry, Southern Federal University, Rostov-on-Don, Russia
[2]The Smart Materials Research Institute, Southern Federal University, Rostov-on-Don, Russia
[3]Federal Research Centre the Southern Scientific Center of the Russian Academy of Sciences, Rostov-on-Don, Russia
[4]Advanced Functional Materials & Optoelectronic Laboratory (AFMOL), Department of Physics, Faculty of Science, King Khalid University, Abha, Saudi Arabia
[5]Metallurgical Lab., Nanoscience Laboratory for Environmental and Bio-medical Applications (NLEBA), Semiconductor Lab., Physics Department, Faculty of Education, Ain Shams University, Roxy, Cairo, Egypt

$BiMnO_3$ exhibit multiferroic properties, which attract much attention due to numerous potential applications. The most well-investigated and traditional techniques for synthesizing this material include high-pressure and high-temperature treatment. In this way, soft chemistry synthesis of $BiMnO_3$ is desirable. Even though the formation of $BiMnO_3$ at ambient pressure is not possible according to the phase diagram, many scientific groups are focused on solving this problem. In the present work, we have

Address correspondence to Vera V. Butova, The Smart Materials Research Institute, Southern Federal University, Rostov-on-Don, Russia. E-mail: vbutova@sfedu.ru

Color versions of one or more of the figures in the article can be found online at www.tandfonline.com/gcic.

tested four soft chemistry routes, namely hydrothermal route, two gel methods, and coprecipitation for synthesizing $BiMnO_3$ from $Cl^-$ and $NO_3^-$-containing solutions at ambient pressure in the temperature range of 200–800°C, and none resulted in the formation of $BiMnO_3$. The experiment showed that under hydrothermal conditions manganese and bismuth oxides remain unreacted, and the other tested methods produce $Bi_2Mn_4O_{10}$ and $Bi_{12}MnO_{20}$ instead. The formation of $Bi_2Mn_4O_{10}$ and $Bi_{12}MnO_{20}$ from $Cl^-$-containing solutions occurs with BiOCl being formed as an intermediate phase.

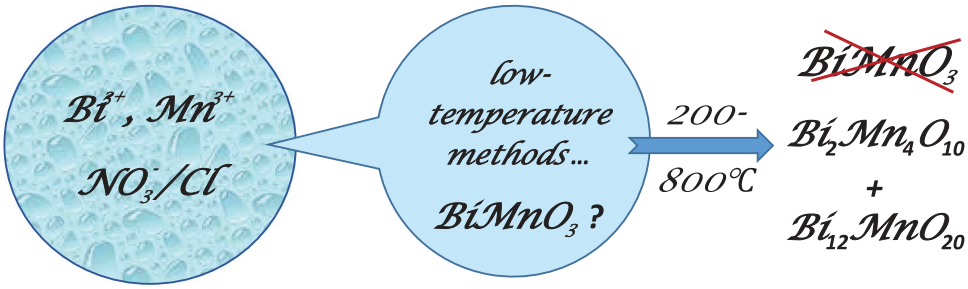


**Keywords** Multiferroics, bismuth manganite, low-temperature synthesis, phase transformations

## 1. INTRODUCTION

Bismuth manganite ($BiMnO_3$) belongs to the group of multiferroic materials which have drawn significant attention in recent years.[1–3] In multiferroic materials, (anti)ferroelectric, (anti)ferromagnetic, and ferroelastic properties coexist in the same phase.[4,5] Among perovskite-type manganites of the general formula $AMnO_3$ (A = massive trivalent cation, typically lanthanum or lanthanide), $BiMnO_3$ is a rare example of the compound with ferromagnetic ordering.[6] Ferromagnetism in $BiMnO_3$ is observed below its $T_C \approx -170$°C due to the unusual orbital ordering that stems from the steric effect of the $6s^2$ lone-pair on the $Bi^{3+}$ cation.

The theoretical calculations[7] suggested that $BiMnO_3$ can show both ferromagnetic and ferroelectric ordering.[8] The lone-pair on $Bi^{3+}$ is also believed to be the origin of ferroelectricity in $BiMnO_3$, but some of the structural properties contradict ferroelectric ordering. Initially, the structure of perovskite-type $BiMnO_3$ was considered as triclinic[9,10], but the further experiments showed that metastable $BiMnO_3$ crystallizes in noncentrosymmetric monoclinic space group C2 at ambient temperature and pressure[11–13] (Figure 1). In subsequent studies[14,15], it was suggested that $BiMnO_3$ has a centrosymmetric structure belonging to space group C2/c, which is

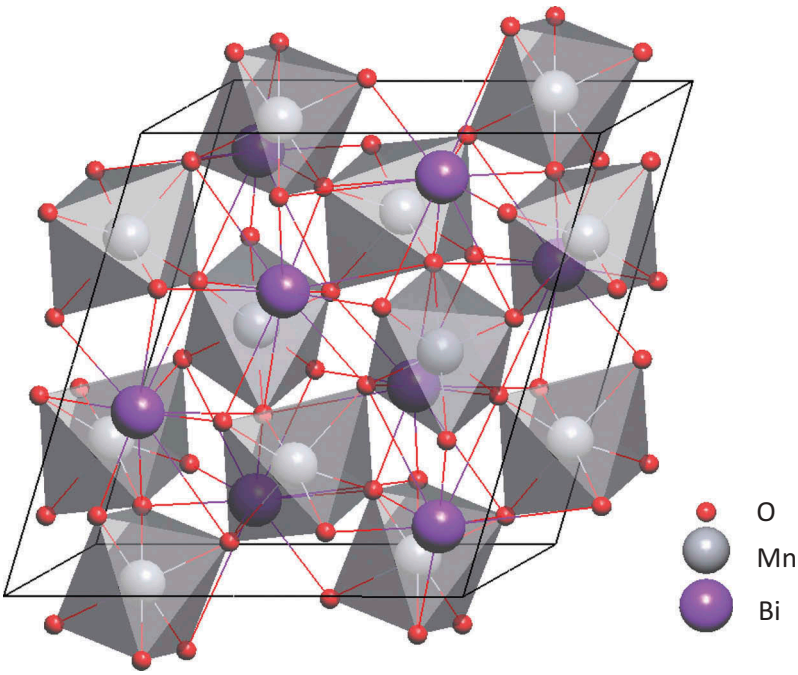


**Figure 1:** Structure model of monoclinically distorted $BiMnO_3$.

confirmed by calculations[16], but inconsistent with ferroelectricity. These observations continue to be the subject of discussion.[17]

Structural transformations in $BiMnO_3$ highly depend on the external conditions (T, P). At ~500°C, $BiMnO_3$ undergoes monoclinic-to-orthorhombic phase transition and crystallizes in space group Pnma, becoming isostructural with $LaMnO_3$.[18,19] High-pressure experiments[20] showed two phase transitions: the first one at 1 GPa originates from a change in $MnO_6$ cooperative octahedral tilting (monoclinic space group P21/c), and at 6 GPa the symmetry increases up to orthorhombic (Pnma).

It is a commonly known fact that stabilized perovskite-type bismuth manganite can be synthesized only at high pressures.[21] And indeed, the phase diagram for the system Bi – Mn – O[22,23] shows that only two compounds, $Bi_2Mn_4O_{10}$ and $Bi_{12}MnO_{20}$ (or pure $Bi_2O_3$), could be formed at ambient pressure. In manganese sillenite $Bi_{12}MnO_{20}$, the $Mn^{4+}$ cations form isolated $[MnO_4]$ tetrahedra incorporated in three-dimensional network of $[BiO_5]$ square pyramids. In $Bi_2Mn_4O_{10}$, $Bi^{3+}$ occupies highly distorted octahedral sites, $Mn^{3+}$ and $Mn^{4+}$ occupy pyramidal and octahedral sites, respectively, in the ratio 1:1. Corner- and edge-sharing coordination polyhedra of Mn and Bi assemble two three-dimensional-interconnected networks.

Perovskite-type $BiMnO_3$ cannot be synthesized at ambient pressure according to the phase diagram.

The first synthesis of perovskite $BiMnO_3$ was reported in 1965–1968.[9,10,24] Mixture of $Bi_2O_3$ and $Mn_2O_3$ was placed in a graphite capsule, which also acted as a heater, and reacted at 40 kbar and 700°C for 30–60 min before quenching. When heated to 300–600°C at ambient pressure, metastable perovskite $BiMnO_3$ decomposes into $Bi_2Mn_4O_{10}$ and $Bi_2O_3$ (or $Bi_{12}MnO_{20}$).[18]

While high-pressure treatment continues to be an effective method to produce bismuth manganite from oxides[14,15,20,25–29], various soft chemical routes were recently attempted for the synthesis of perovskite-type $BiMnO_3$ at low temperature and pressure.[30–35] The synthesis of bismuth manganite from the chloride solution by coprecipitation with NaOH at 100–120°C was reported in.[30,34] Hydrothermal synthesis of $BiMnO_3$ from chloride solution was attempted by Sun et al.[33], the product was a thin film on a titanium substrate. Acharya et al.[35] reported a hydrothermal synthesis of fine powder $BiMnO_3$ from nitrate and acetate solutions at 180°C and 40 MPa. Mazumder et al. described an original approach of producing $BiMnO_3$ biogenically using fungal biomass.[31] In this method, freshly prepared bismuth and manganese hydroxides were heated at 100°C for 12 h; the fungal biomass was cultivated separately at 50°C and pH = 9 for four days. For "bio-milling" of synthesized particles, the fungal mycelium was suspended in a hydroxide medium.

All the above wet-chemical methods appear promising as an alternative for classical methods that require expensive equipment for high-pressure synthesis and long heating. However, the reported powder X-ray diffraction (XRD) data[30–35] could not be associated with successful low-pressure synthesis. Moreover, recently Sun et al. retracted their original paper[33] and provided a notice with explanation.[36] In a follow-up study,[36] Sun et al. repeated the hydrothermal synthesis from Bi, Mn, Cl-containing aqueous solution on the Ti substrate according to their previously reported method[33] and compared the XRD pattern of the product with the standard XRD patterns of $BiMnO_3$ (JCPDS 89–4544) and BiOCl (JCPDS 82–0485). The authors have found that the pattern of synthesized material agrees well with BiOCl instead of $BiMnO_3$. Moreover, the pattern displayed the peaks attributed to Ti substrate and three additional peaks of unidentified phase ($2\Theta$ = 30.35, 42.40 and 57.00). The XRD pattern of the same material reported in the original paper[33] do not show any additional peaks and is in good agreement with JCPDS 82–0485 (BiOCl). The analogical XRD patterns consistent with JCPDS 82–0485 (BiOCl) were reported in a number of papers[30,31,35] being incorrectly interpreted as the pattern of $BiMnO_3$. In this regard, the XRD patterns of pure $BiMnO_3$ product without any additional phases reported by Hanif et al.[34] look surprising and

conflict with other studies[30,31,35] that deal with almost the same synthesis method.[30,31]

The present study was undertaken to test various soft chemistry methods for synthesizing $BiMnO_3$ from $NO_3^-$ (methods a) and $Cl^-$ (methods b) solutions at ambient pressure. The first group of tested methods (methods 1a-b) is hydrothermal routes. The second group is gel methods (methods 2a-b) based on the Pechini process[37], which starts with introducing salts or metal alkoxides into a solution of citric acid in ethylene glycol or glycerin. In the third group of methods (methods 3a-b), aqueous solutions of polyvinyl alcohol (PVA) are used as a polymer medium. Previously we have successfully used PVA-assisted gel method to produce a number of magnetic and multiferroic materials.[38–42] And, finally, methods 4a-b are coprecipitation routes.

## 2. MATERIALS AND METHODS

In methods 1a-b, bismuth oxide was dissolved in nitric (method 1a) or hydrochloric acid (method 1b), required amount of manganese (II) nitrate (method 1a) or chloride (method 1b) was then added into solution. Manganese content was determined gravimetrically by precipitation of manganese ammonium phosphate.[43] The resulted solution was added dropwise into 40% NaOH with stirring, 3% $H_2O_2$ was added to oxidize Mn (II). The final mixture was loaded in a Teflon autoclave reactor and hydrothermally treated at 200°C and 3 MPa for ~24 h. The resulted product was washed with distilled water to pH = 7 and dried at ~100°C.

In the Pechini method[37], metal chelates undergo polyesterification with a polyfunctional alcohol to form polymer gel. In methods 2a-b, citric acid and glycerin were added to mixed $Bi^{3+}$- and $Mn^{2+}$-containing nitric (method 2a) or hydrochloric acid (method 2b) solutions in the molar ratio, citric acid:metal ion = 3:1, glycerin:citric acid = 1:3. The mixture which contained polybasic chelates was concentrated in air at 80–90°C and dried at ~120°C to form xerogels 2a and 2b.

Methods 3a-b involve PVA-assisted gel process.[38–42] Mixed $Bi^{3+}$- and $Mn^{2+}$-containing nitric (method 3a) or hydrochloric acid (method 3b) solutions were added dropwise into aqueous PVA solution with stirring. Heating the mixture at 80–90°C in air and drying yielded xerogels 3a and 3b.

In methods 4a-b, mixed $Bi^{3+}$- and $Mn^{2+}$-containing nitric (method 4a) or hydrochloric acid (method 4b) solutions were added slowly dropwise into excess concentrated ammonia solution with stirring, an excess of $H_2O_2$ was then added to oxidize Mn(II). The resulted precipitates 4a and 4b were filtered and washed thoroughly with distilled water to pH = 7.

The xerogels made by methods 2a, 2b, 3a, 3b, and precipitates 4a and 4b were calcined in the temperature range of 200–800°C with a step size of 100° C.

X-ray powder diffraction (XRD) was carried out using an ARL-X'TRA diffractometer ($CuK_\alpha$ radiation).

Xerogels 2a, 2b, 3a, 3b, and precipitates 4a and 4b were characterized by thermogravimetric analysis (TGA) and differential scanning calorimetry (DSC) using an STA 449 F3 Jupiter simultaneous thermal analyzer equipped with a QMS 403C Aeolos Quadro quadrupole mass spectrometer. The specimens were placed into the $Al_2O_3$ crucibles and heated from 20°C to 800°C in air at a heating rate of 5°/min.

When calcined at 400–600°C, the products of methods 2b, 3b and 4b were analyzed by energy-dispersive X-ray spectroscopy (EDS) using an Oxford Instruments INCA ENERGY 450/XT Microanalysis System equipped with a detector X-Act ADD and INCA WAVE 700 wavelength-dispersive X-ray spectrometer.

## 3. RESULTS AND DISCUSSION

Figure 2 shows the XRD patterns of the samples produced hydrothermally using methods 1a and 1b. In both cases, in addition to the predominant peaks corresponding to $Bi_2O_3$, the patterns show small peaks that can be ascribed to $Bi_{12}MnO_{20}$. Under hydrothermal conditions, manganese forms only rutile-type

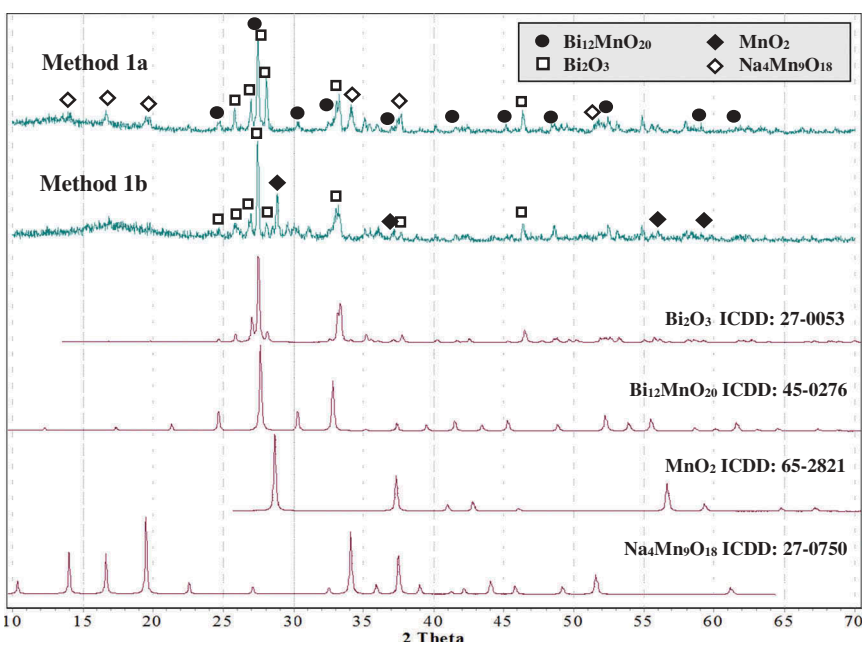


**Figure 2:** XRD patterns of the hydrothermally treated samples prepared by methods 1a and 1b.

$MnO_2$ (method 1b) or its sodium-containing species $Na_4Mn_9O_{18}$ (method 1a). Thus, manganese and bismuth oxides remain unreacted under hydrothermal conditions.

Below we discuss the attempts to synthesize bismuth manganite from $NO_3^-$containing solutions using gel methods 2a and 3a, and coprecipitation method 4a (Figure 3). The products 2a and 4a were amorphous by XRD up to ~300°C. In addition, the samples produced from PVA-based gel appeared containing unidentified crystalline phase. After calcining at 400°C, these samples exhibited diffraction peaks corresponding to bismuth oxide species $Bi_{7.72}Mn_{0.28}O_{12.14}$ known from the literature. The peaks of $Bi_{7.72}Mn_{0.28}O_{12.14}$ appeared at 400°C and then sharpened on treatment at 500°C in parallel with the appearance of unidentified peaks (the major peak is positioned at 2Θ = 27°). In the samples produced by method 2a and 4a, calcining at 400–500°C also yields some crystalline phases, which, however, could not be identified. $Bi_2Mn_4O_{10}$ formation occurred in all samples at 600°C, being accompanied by $Bi_2O_3$-derived phase $Bi_{12}MnO_{20}$ (methods 3a and 4a) and unidentified secondary phase (method 2a). After calcining at 700–800°C, all the samples appeared to be mixtures of $Bi_2Mn_4O_{10}$ and $Bi_{12}MnO_{20}$. There was no significant difference in the XRD patterns of the calcined products, regardless of the method used.

The underlying chemical processes can be represented by the following equations:

**Method 2a**

$$Bi^{3+} + Mn^{2+} + 5NO_3^- + 6_{35}(COOH)_3 + 2C_3H_5(OH)_3 \xrightarrow{100-120^\circ C}$$

$$(H_3O)_5BiMn\left(C_3H_5O(COO)_3\right)_6(C_3H_5)_2 + 5NO_2\uparrow + 4.5H_2O\uparrow + 0.75O_2\uparrow \xrightarrow{+33.88O_2}$$

$$\ldots \xrightarrow{700-800^\circ C} \frac{11}{46}\mathbf{Bi_2Mn_4O_{10}} + \frac{1}{23}\mathbf{Bi_{12}MnO_{20}} + 42CO_2\uparrow + 22.5H_2O\uparrow$$

**Method 3a**

$$Bi^{3+} + Mn^{2+} + 5NO_3^- + (CH_2CHOH)_n \xrightarrow{100-120^\circ C}$$

$$Bi(NO_3)_3 \times Mn(NO_3)_2 \times (CH_2CHOH)_n \xrightarrow{+12.13O_2}$$

$$\ldots \xrightarrow{700-800^\circ C} \frac{11}{46}\mathbf{Bi_2Mn_4O_{10}} + \mathbf{Bi_{12}MnO_{20}} + 10CO_2\uparrow + 5NO_2\uparrow + 10\,H_2O\uparrow$$

**Method 4a**

$$Bi^{3+} + Mn^{2+} + 5OH^- + H_2O_2 + (x + 0.5y - 3.5)\,H_2O \xrightarrow{20^\circ C}$$

$$MnO_2 \times xH_2O + 0.5Bi_2O_3 \times yH_2O \rightarrow \ldots$$

$$\xrightarrow{700-800^\circ C} \frac{11}{46}Bi_2Mn_4O_{10} + \frac{1}{23}Bi_{12}MnO_{20} + \frac{11}{92}O_2\uparrow + (x + 0.5y)\,H_2O\uparrow$$

When attempting to synthesize $BiMnO_3$ from $Cl^-$containing solutions using methods 2b, 3b, and 4b, in the latter two cases bismuth oxychloride

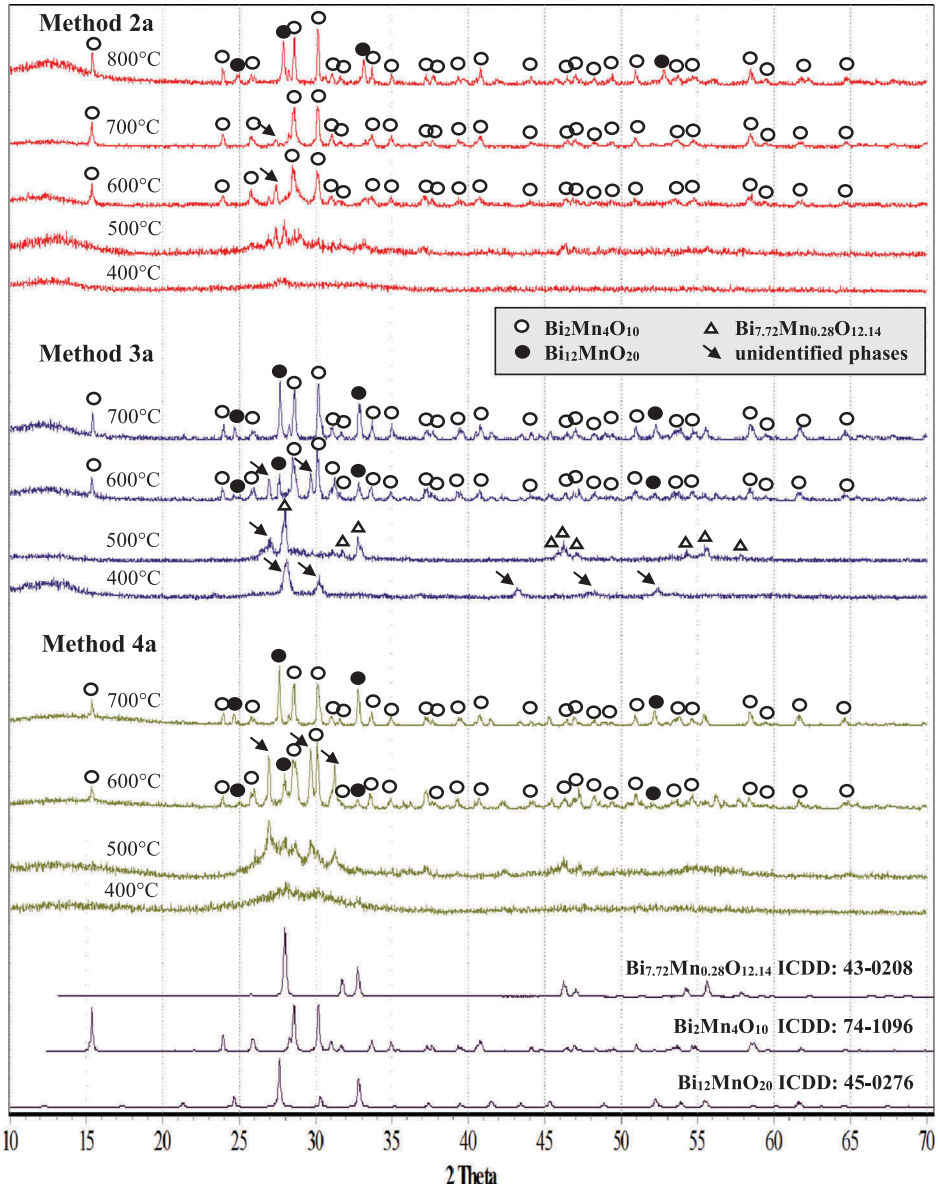


**Figure 3:** XRD patterns illustrating phase transformations during synthesis of bismuth manganite from $NO_3^-$-containing solutions using methods 2a, 3a, and 4a.

BiOCl formed after treatment at 180–200°C and remained the only crystalline phase up to 400–500°C (Figure 4). In method 2b, the sample dried at 200°C was amorphous, and after treatment at 300°C, in spite the fact that the sample was calcined in air, the peaks of metallic Bi appeared in XRD patterns,

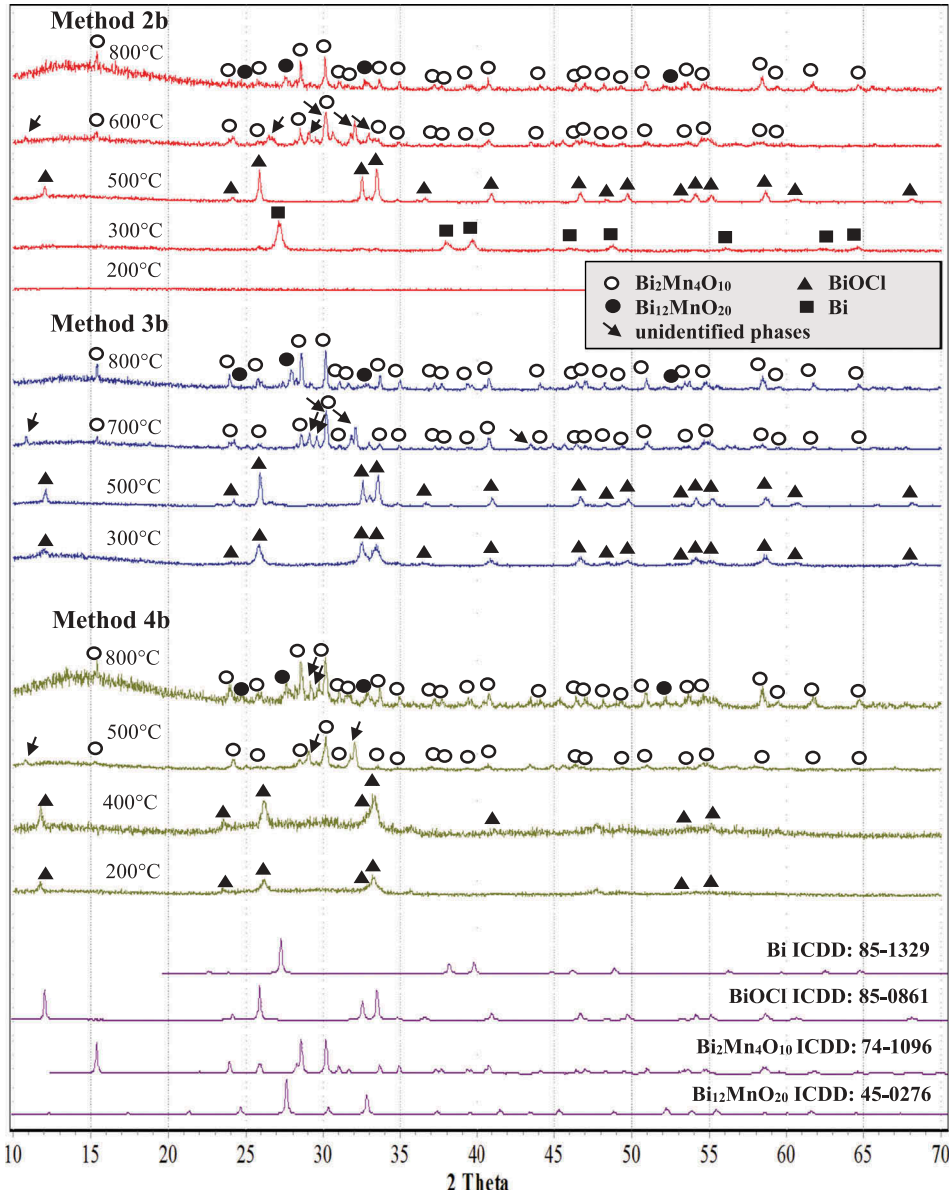


**Figure 4:** XRD patterns illustrating phase transformations during synthesis of bismuth manganite from $Cl^-$containing solutions using methods 2b, 3b, and 4b.

suggesting reduction of $Bi^{3+}$ by decomposing organic components of the xerogel. BiOCl, which is reported to be thermally stable at temperatures below 595°C[44], was observed to stabilize in this system as the calcining temperature increases up to 400–500°C. Therefore, heating the samples to 600–700°C

decomposed this phase, producing $Bi_2Mn_4O_{10}$ in all three cases. Finally, calcining at 800°C yielded a mixture of $Bi_2Mn_4O_{10}$ and $Bi_{12}MnO_{20}$. The reactions can be written as:

**Method 2b**

$$Bi^{3+}+Mn^{2+}+5Cl^{-}+3_{35}(COOH)_3+C_3H_5(OH)_3+0.5O_2 \xrightarrow{100-120^\circ C}$$

$$(H_3O)_2Mn\left(C_3H_5O(COO)_3\right)_3(C_3H_5)+BiOCl+4HCl\uparrow+2H_2O\uparrow \xrightarrow{+16.88O_2}$$

$$\ldots \xrightarrow{700-800^\circ C} \frac{11}{46}\mathbf{Bi_2Mn_4O_{10}}+\frac{1}{23}\mathbf{Bi_{12}MnO_{20}}+21CO_2\uparrow+HCl\uparrow+10.5H_2O\uparrow$$

**Method 3b**

$$Bi^{3+}+Mn^{2+}+5Cl^{-}+(CH_2CHOH)_n+H_2O \xrightarrow{100-120^\circ C}$$

$$\mathbf{BiOCl}\cdot MnCl_2\times\frac{5}{n}(CH_2CHOH)_n+2HCl\uparrow \xrightarrow{+12.88O_2}$$

$$\ldots \xrightarrow{700-800^\circ C} \frac{11}{46}Bi_2Mn_4O_{10}+\frac{1}{23}Bi_{12}MnO_{20}+10CO_2\uparrow+3HCl\uparrow+8.5H_2O\uparrow$$

**Method 4b**

$$Bi^{3+}+Mn^{2+}+Cl^{-}+4OH^{-}+H_2O_2+(x-2)H_2O\cdot \xrightarrow{20^\circ C}$$

$$BiOCl+MnO_2\cdot xH_2O\rightarrow$$

$$\ldots \xrightarrow{700-800^\circ C} \frac{11}{46}\mathbf{Bi_2Mn_4O_{10}}+\frac{1}{23}\mathbf{Bi_{12}MnO_{20}}+\frac{11}{92}O_2\uparrow+HCl\uparrow+(x-0.5)H_2O\uparrow$$

BiOCl occurs as an intermediate phase during the formation of manganites $Bi_2Mn_4O_{10}$ and $Bi_{12}MnO_{20}$. The typical EDS spectrum (Figure 5, the sample produced by method 2 after calcining at 500°C) shows the atomic ratio Bi:Cl of close to 1:1, indicating incorporation of bismuth into BiOCl, which agrees with XRD observations.

Results from the XRD analysis of the products synthesized using all tested methods are summarized in Table 1.

TGA and DSC curves of the samples produced by methods 2a, 2b and 3a, 3b refer to the complex processes initiated by organic residues (Figure 6, curve 1, 2, 1′, and 2′). Thermal behaviors of all the products share common features and will be discussed further in the case of samples synthesized by

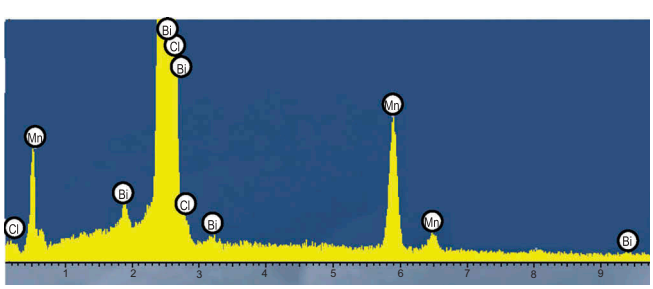


| Element | at.% |
|---|---|
| Bi | 35.7 |
| Mn | 32.9 |
| Cl | 31.4 |

**Figure 5:** EDS spectrum of the sample produced by method 2b after calcining at 500°C.

**Table 1:** A summary of the phases observed by XRD at various heating temperatures for all tested methods.

| | Additive | $Bi^{3+}$ source | $Mn^{2+}$ source | Heat treatment temperature, °C | Phases |
|---|---|---|---|---|---|
| Method **1a** | NaOH | $Bi_2O_3$ + $HNO_3$ | $Mn(NO_3)_2$ | 200 | $Bi_2O_3$, small amount of $Bi_{12}MnO_{20}$, $Na_4Mn_9O_{18}$ |
| Method **2a** | citric acid and glycerin | | | 200–400 | amorph.* |
| | | | | 500 | U.P.** + amorph. |
| | | | | 600, 700 | $Bi_2Mn_4O_{10}$ + U.P. |
| | | | | 800 | $Bi_2Mn_4O_{10}$ + $Bi_{12}MnO_{20}$ |
| Method **3a** | aqueous solutions of PVA | | | 200–300 | amorph. |
| | | | | 400 | U.P. + amorph. |
| | | | | 500 | $Bi_{7.72}Mn_{0.28}O_{12.14}$ + U.P. |
| | | | | 600 | $Bi_2Mn_4O_{10}$ + $Bi_{12}MnO_{20}$ + U.P |
| | | | | 700 | $Bi_2Mn_4O_{10}$ + $Bi_{12}MnO_{20}$ |
| Method **4a** | NaOH | | | 200–400 | amorph. |
| | | | | 500 | U.P. + amorph. |
| | | | | 600 | $Bi_2Mn_4O_{10}$ + $Bi_{12}MnO_{20}$ + U.P |
| | | | | 700 | $Bi_2Mn_4O_{10}$ + $Bi_{12}MnO_{20}$ |
| Method **1b** | NaOH | $Bi_2O_3$ + HCl | $MnCl_2$ | 200 | $Bi_2O_3$, small amount of $Bi_{12}MnO_{20}$, $MnO_2$ |
| Method **2b** | citric acid and glycerin | | | 200 | amorph. |
| | | | | 300 | Bi |
| | | | | 400–500 | BiOCl |
| | | | | 600 | $Bi_2Mn_4O_{10}$ + U.P. |
| | | | | 700–800 | $Bi_2Mn_4O_{10}$ + $Bi_{12}MnO_{20}$ |
| Method **3b** | aqueous solutions of PVA | | | 200–600 | BiOCl |
| | | | | 700 | $Bi_2Mn_4O_{10}$ + U.P. |
| | | | | 800 | $Bi_2Mn_4O_{10}$ + $Bi_{12}MnO_{20}$ |
| Method **4b** | NaOH | | | 200–600 | BiOCl |

(*Continued*)

**Table 1:** (*Continued*).

| Additive | $Bi^{3+}$ source | $Mn^{2+}$ source | Heat treatment temperature, °C | Phases |
|---|---|---|---|---|
| | | | 700 | $Bi_2Mn_4O_{10}$ + U.P. |
| | | | 800 | $Bi_2Mn_4O_{10}$ + $Bi_{12}MnO_{20}$ |

*amorph. – Amorphous phase;
**U.P. - Unidentified phase.

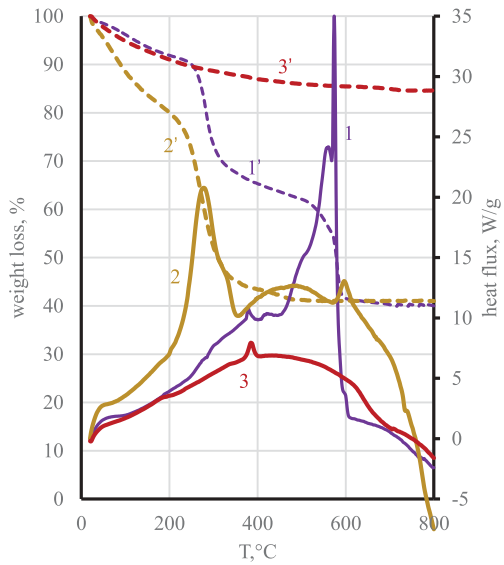


**Figure 6:** DSC (solid) and TGA (dashed) curves for the samples produced by methods 2a (curves 1 and 1'), 2b (2 and 2'), 4b (3 and 3').

the Pechini route (method 2a and 2b). For the xerogel produced from $NO_3^-$ containing solution (method 2a), a sharp weight loss associated with a series of exothermic effects occurs in the temperature range from 200°C to 300°C, which can be explained by the organic burnout. This complete and rapid burnout is likely supported by the high oxidizing power of $NO_3^-$ ions. No further weight loss appeared in continuing the heating over 300°C. The high exotherm at ~600°C indicates that $Bi_2Mn_4O_{10}$ is formed, as seen by XRD. Further, two comparatively smaller exothermic peaks appeared at 670°C and 735°C due to transformations of $Bi_2O_3$-derived phases. For the xerogel produced from $Cl^-$containing solution (method 2b), the first sharp weight loss corresponding to the organic burnout occurs in the temperature range of

~260–320°C. An unexplained exothermic effect was observed at 380°C. Two exothermic peaks at 560°C and 580°C are associated with the second sharp weight loss, and on further heating the weight is constant. The XRD patterns indicate that BiOCl decomposes near these temperatures, which could be due to reaction with air. We propose two possible explanations: the oxidation by oxygen

$$BiOCl_{(s)} + \frac{1}{4}O_{2(g)} \rightarrow \frac{1}{2}Bi_2O_{3(s)} + \frac{1}{2}Cl_{2(g)},$$

$\Delta H°_{298}$ = 88.7 kJ/mol, $\Delta S°_{298}$ = 187.2 J/(mol·K)
and, alternatively, the high-temperature hydrolysis

$$BiOCl_{(s)} + \frac{1}{2}H_2O_{(g)} \rightarrow \frac{1}{2}Bi_2O_{3(s)} + HCl_{(g)},$$

$\Delta H°_{298}$ = 117.4 kJ/mol, $\Delta S°_{298}$ = 65.7 J/(mol·K).

The calculation of thermodynamic quantities (the constants are taken from reference[45]) shows that both reactions are endothermic and driven by a gain in entropy. Thus, the only possible reason behind the exothermic effects observed in this temperature range is the organic burnout, and the released heat facilitates the formation of $Bi_2O_3$ phases from BiOCl.

Samples 4a and 4b, which contain no organic matter, show no effects similar to those occurring with products of methods 1–3, as exemplified in Figure 6 (curve 3 and 3′) by TGA and DSC curves for a chloride-derived precipitate (method 4b). In the temperature range of 100–800°C, TGA shows gradual weight loss due to moisture evaporation and outgassing of other volatiles. Additionally, the DSC curve shows an unexplained exothermic effect at ~390°C.

## 4. CONCLUSION

From the experiments, it appeared that $BiMnO_3$ cannot be synthesized from $NO_3^-$ and $Cl^-$-containing solutions using hydrothermal route, coprecipitation, and gel methods. Under hydrothermal conditions, manganese and bismuth oxides remain unreacted, and the other methods produce $Bi_2Mn_4O_{10}$ and $Bi_{12}MnO_{20}$ instead, which agrees with the phase diagram for the system Bi – Mn – O. The formation of $Bi_2Mn_4O_{10}$ and $Bi_{12}MnO_{20}$ from $Cl^-$containing solutions occurs with BiOCl being formed as an intermediate phase.

## ACKNOWLEDGMENTS

We thank Dr. Yu. V. Popov and N. A. Avtushenko (Share Research Centre "Centre for Research of Mineral Resources and the Environment", Institute of Earth Sciences, Southern Federal University) for thermal and elemental analysis. The authors express their appreciation to the Deanship of Scientific Research at King Khalid University for funding this work through research groups program under grant number R.G.P.1/12/39.

## DISCLOSURE STATEMENT

No potential conflict of interest was reported by the authors.

## FUNDING

This work was supported by the the Deanship of Scientific Research at King Khalid University [R.G.P.1/12/39].

## ORCID

Inna V. Lisnevskaya http://orcid.org/0000-0002-2069-8990
Vera V. Butova http://orcid.org/0000-0002-4099-0737

## REFERENCES

[1] Belik, A. A.;. Polar and Nonpolar Phases of $BiMO_3$: A Review. *J. Solid State Chem.* **2012**, 195, 32–40. DOI: 10.1016/j.jssc.2012.01.025.

[2] Kundu, A. K.; Seikh, M. M.; Nautiyal, P. Bismuth Centred Magnetic Perovskite: A Projected Multiferroic. *J. Magn. Magn. Mater.* **2015**, 378, 506–528. DOI: 10.1016/j.jmmm.2014.11.044.

[3] Molak, A.; Mahato, D. K.; Szeremeta, A. Z. Synthesis and Characterization of Electrical Features of Bismuth Manganite and Bismuth Ferrite: Effects of Doping in Cationic and Anionic Sublattice: Materials for Applications. *Prog. Cryst. Growth Charact. Mater.* **2018**, 64, 1–22. DOI: 10.1016/j.pcrysgrow.2018.02.001.

[4] Tokunaga, M.; Hakuta, S.; Tamegai, T. Electronic States in Polycrystalline and Crystalline Bismuth-based Manganites. *J. Magn. Magn. Mater.* **2007**, 310, 885–887. DOI: 10.1016/j.jmmm.2006.10.1100.

[5] Yang, C. H.; Koo, T. Y.; Jeong, Y. H. Orbital Order, Magnetism, and Ferroelectricity of Multiferroic $BiMnO_3$. *J. Magn. Magn. Mater.* **2007**, 310, 1168–1170. DOI: 10.1016/j.jmmm.2006.10.278.

[6] Gonchar, L. E.;. Orbital State Dependence of Insulating Manganites' Magnetic Ordering. *J. Magn. Magn. Mater.* **2018**, 465, 661–669. DOI: 10.1016/j.jmmm.2018.06.012.

[7] Hill, N. A.; Rabe, K. M. First-principles Investigation of Ferromagnetism and Ferroelectricity in Bismuth Manganite. *Phys. Rev. B.* **1999**, 59, 8759–8769. DOI: 10.1103/PhysRevB.59.8759.

[8] Zhai, L. J.; Wang, H. Y. The Magnetic and Multiferroic Properties in $BiMnO_3$. *J. Magn. Magn. Mater.* **2017**, 426, 188–194. DOI: 10.1016/j.jmmm.2016.11.065.

[9] Sugawara, F.; Iida, S.; Syono, Y.; Akimoto, S.-I. New Magnetic Perovskites $BiMnO_3$ and BiCrO3. *J. Phys. Soc. Jpn.* **1965**, 20, 1529. DOI: 10.1143/JPSJ.20.1529.

[10] Sugawara, F.; Iiida, S.; Syono, Y.; Akimoto, S.-I. Magnetic Properties and Crystal Distortions of $BiMnO_3$ and $BiCrO_3$. *J. Phys. Soc. Jpn.* **1968**, 25, 1553–1558. DOI: 10.1143/JPSJ.25.1553.

[11] Atou, T.; Chiba, H.; Ohoyama, K.; Yamaguchi, Y.; Syono, Y. Structure Determination of Ferromagnetic Perovskite BiMnO3. *J. Solid State Chem.* **1999**, 145, 639–642. DOI: 10.1006/jssc.1999.8267.

[12] Kimura, T.; Kawamoto, S.; Yamada, I.; Azuma, M.; Takano, M.; Tokura, Y. Magnetocapacitance Effect in Multiferroic $BiMnO_3$. *Phys. Rev. B.* **2003**, 67. DOI: 10.1103/PhysRevB.67.180401.

[13] Chi, Z. H.; Xiao, C. J.; Feng, S. M.; Li, F. Y.; Jin, C. Q.; Wang, X. H.; Chen, R. Z.; Li, L. T. Manifestation of Ferroelectromagnetism in Multiferroic $BiMnO_3$. *J. Appl. Phys.* **2005**, 98. DOI: 10.1063/1.2131193.

[14] Belik, A. A.; Iikubo, S.; Yokosawa, T.; Kodama, K.; Igawa, N.; Shamoto, S.; Azuma, M.; Takano, M.; Kimoto, K.; Matsui, Y.; et al. Origin of the Monoclinic-to-monoclinic Phase Transition and Evidence for the Centrosymmetric Crystal Structure of $BiMnO_3$. *J. Am. Chem. Soc.* **2007**, 129, 971–977. DOI: 10.1021/ja0664032.

[15] Montanari, E.; Calestani, G.; Righi, L.; Gilioli, E.; Bolzoni, F.; Knight, K. S.; Radaelli, P. G. Structural Anomalies at the Magnetic Transition in Centrosymmetric $BiMnO_3$. *Phys. Rev. B.* **2007**, 75. DOI: 10.1103/PhysRevB.75.220101.

[16] Baettig, P.; Seshadri, R.; Spaldin, N. A. Anti-polarity in Ideal $BiMnO_3$. *J. Am. Chem. Soc.* **2007**, 129, 9854. DOI: 10.1021/ja073415u.

[17] Solovyev, I. V.; Pchelkina, Z. V. Magnetic-field Control of the Electric Polarization in $BiMnO_3$. *Phys. Rev. B.* **2010**, 82. DOI: 10.1103/PhysRevB.82.094425.

[18] Faqir, H.; Chiba, H.; Kikuchi, M.; Syono, Y.; Mansori, M.; Satre, P.; Sebaoun, A. High-temperature XRD and DTA Studies of BiMnO3 Perovskite. *J. Solid State Chem.* **1999**, 142, 113–119. DOI: 10.1006/jssc.1998.7994.

[19] Sundaresan, A.; Mangalam, R. V. K.; Iyo, A.; Tanaka, Y.; Rao, C. N. R. Crucial Role of Oxygen Stoichiometry in Determining the Structure and Properties of $BiMnO_3$. *J. Mater. Chem.* **2008**, 18, 2191–2193. DOI: 10.1039/b803118p.

[20] Calestani, G.; Orlandi, F.; Mezzadri, F.; Righi, L.; Merlini, M.; Gilioli, E. Structural Evolution under Pressure of $BiMnO_3$. *Inorg. Chem.* **2014**, 53, 8749–8754. DOI: 10.1021/ic5013878.

[21] Rooymans, C. J. M. High-Pressure Techniques in Preparative Chemistry. In *Preparative Methods in Solid State Chemistry*; Hagenmuller, P., Ed.; Academic Press: New York & London, 1972; pp 71–132.

[22] Phase Equilibria Diagram Database. *Version 3.1*; ACerS - NIST, The American CeramicSociety Customer Service Department: Westerville, OH, 2006. Fig. 00027 E.

[23] Havelia, S.; Wang, S.; Skowronski, M.; Salvador, P. A. Controlling the Bi Content, Phase Formation, and Epitaxial Nature of BiMnO3 Thin Films Fabricated Using Conventional Pulsed Laser Deposition, Hybrid Pulsed Laser Deposition, and Solid State Epitaxy. *J. Appl. Phys.* **2009**, 106. DOI: 10.1063/1.3266142.

[24] Tomashpolski, Y. Y.; Zubova, E. B.; Burdina, K. P.; Venevtcev, Yu. N. X-ray Diffraction Study of New Perovskites Produced at High Pressures. *Kristallografiya*. **1968**, 13, 987–990.

[25] Yang, H.; Chi, Z. H.; Jiang, J. L.; Feng, W. J.; Cao, Z. E.; Xian, T.; Jin, C. Q.; Yu, R. C. Centrosymmetric Crystal Structure of $BiMnO_3$ Studied by Transmission Electron Microscopy and Theoretical Simulations. *J. Alloy. Compd.* **2008**, 461, 1–5. DOI: 10.1016/j.jallcom.2007.06.085.

[26] Toulemonde, P.; Darie, C.; Goujon, C.; Legendre, M.; Mendonca, T.; Alvarez-Murga, M.; Simonet, V.; Bordet, P.; Bouvier, P.; Kreisel, J.; et al. Single Crystal Growth of $BiMnO_3$ under High Pressure-high Temperature. *High Pressure Res.* **2009**, 29, 600–604. DOI: 10.1080/08957950903467050.

[27] Belik, A. A.; Kolodiazhnyi, T.; Kosuda, K.; Takayama-Muromachi, E. Synthesis and Properties of Oxygen Non-stoichiometric $BiMnO_3$. *J. Mater. Chem.* **2009**, 19, 1593–1600. DOI: 10.1039/b818645f.

[28] Belik, A. A.; Yusa, H.; Hirao, N.; Ohishi, Y.; Takayama-Muromachi, E. Peculiar High-Pressure Behavior of BiMnO3. *Inorg. Chem.* **2009**, 48, 1000–1004. DOI: 10.1021/ic8015996.

[29] Kozlenko, D. P.; Dang, N. T.; Jabarov, S. H.; Belik, A. A.; Kichanov, S. E.; Lukin, E. V.; Lathe, C.; Dubrovinsky, L. S.; Kazimirov, V. Y.; Smirnov, M. B.; et al. Structural Polymorphism in Multiferroic $BiMnO_3$ at High Pressures and Temperatures. *J. Alloy. Compd.* **2014**, 585, 741–747. DOI: 10.1016/j.jallcom.2013.10.020.

[30] Samuel, V.; Navale, S. C.; Jadhav, A. D.; Gaikwad, A. B.; Ravi, V. Synthesis of Ultrafine $BiMnO_3$ Particles at 100 Degrees C. *Mater. Lett.* **2007**, 61, 1050–1051. DOI: 10.1016/j.matlet.2006.06.046.

[31] Mazumder, B.; Uddin, I.; Khan, S.; Ravi, V.; Selvraj, K.; Poddar, P.; Ahmad, A. Bio-milling Technique for the Size Reduction of Chemically Synthesized $BiMnO_3$ Nanoplates. *J. Mater. Chem.* **2007**, 17, 3910–3914. DOI: 10.1039/b706154d.

[32] Tarasenko, T. N.; Kravchenko, Z. F.; Kamenev, V. I.; Galyas, A. I.; Demidenko, O. F.; Ignatenko, O. V.; Makoveczki, G. I.; Yanushkevich, K. I. Kristallicheskaya Struktura I Magnitnye Svojstva Nanorazmernyh Poroshkov I Plenok Mul'tiferroika $BiMnO_3$: Vliyanie Davleniya I Zameshcheniya Lantanom [Crystal structure and magnetic properties of nanosized powders and films of multiferroic $BiMnO_3$: the influence of pressure and substitution by lanthanum]. *Fizika I Tehnika Vysokih Davlenij.* **2010**, 20, 70–79.

[33] Sun, B.; Li, C. M. RETRACTED: Light-controlled Resistive Switching Memory of Multiferroic $BiMnO_3$ Nanowire Arrays (retracted Article. See Vol. 19, Pg. 10699, 2017). *Phys. Chem. Chem. Phys.* **2015**, 17, 6718–6721. DOI: 10.1039/c4cp04901b.

[34] Hanif, S.; Hassan, M.; Riaz, S.; Atiq, S.; Hussain, S. S.; Naseem, S.; Murtaza, G. Structural, Magnetic, Dielectric and Bonding Properties of $BiMnO_3$ Grown by Co-precipitation Technique. *Results Phys.* **2017**, 7, 3190–3195. DOI: 10.1016/j.rinp.2017.08.061.

[35] Acharya, S. A.; Gaikwad, V. M.; Kulkarni, S. K.; Despande, U. P. Low Pressure Synthesis of $BiMnO_3$ Nanoparticles: Anomalous Structural and Magnetic Features. *J. Mater. Sci.* **2017**, 52, 458–466. DOI: 10.1007/s10853-016-0345-2.

[36] Li, C. M.;. RETRACTION: Light-controlled Resistive Switching Memory of Multiferroic $BiMnO_3$ Nanowire Arrays (retraction of Vol 17, Pg 6718, 2015). *Phys. Chem. Chem. Phys.* **2017**, 19, 10699–10700. DOI: 10.1039/c7cp90074k.

[37] Pechini, M. P.; Method of Preparing Lead and Alkaline Earth Titanates and Niobates and Coating Method Using the Same to Form a Capacitor. Patent US3330697A, United States, **1967**.

[38] Lisnevskaya, I. V.; Petrova, A. V. Low-temperature Synthesis of the Multiferroic Compound $BiFeO_3$. *Inorg. Mater.* **2009**, 45, 930–934. DOI: 10.1134/S0020168509080202.

[39] Lisnevskaya, I. V.; Bobrova, I. A.; Petrova, A. V.; Lupeiko, T. G. Low-temperature Sol-gel Synthesis of Modified Nickel Ferrite. *Russ. J. Inorg. Chem.* **2012**, 57, 474–477. DOI: 10.1134/S0036023612040171.

[40] Lisnevskaya, I. V.; Lupeiko, T. G.; Bimbad, A. S.; Karyukov, E. V. Sol-Gel Synthesis of Pb-La, Ba-La, and Sr-La Manganites. *Inorg. Mater.* **2014**, 50, 1242–1246. DOI: 10.1134/S0020168514120139.

[41] Lisnevskaya, I. V.; Bobrova, I. A.; Lupeiko, T. G. Synthesis of Yttrium Iron Garnet from a Gel Based on Polyvinyl Alcohol. *Russ. J. Inorg. Chem.* **2015**, 60, 437–441. DOI: 10.1134/S0036023615040130.

[42] Lisnevskaya, I. V.; Bobrova, I. A.; Lupeiko, T. G. Synthesis of Magnetic and Multiferroic Materials from Polyvinyl Alcohol-based Gels. *J. Magn. Magn. Mater.* **2016**, 397, 86–95. DOI: 10.1016/j.jmmm.2015.08.084.

[43] Lavrukhina, A. K.; Yukina, L. V. *Analiticheskaya Khimiya Margantsa [analytical Chemistry of Manganese]*; Nauka: Moscow, 1974.

[44] Zimina, G. V.; Rakov, E. G. Vismuta Galogenidy [Bismuth Halides]. In *Khimicheskaya Entsiklopediya* [In *Chemical Encyclopedia*]; Knunyants, I. L.; Zefirov, N. S., Eds.; Sovetskaya Entsiklopediya: Moscow, 1988; pp. 380–381 (v. 1)..

[45] MSU Thermodynamic Database. Version 2. http://www.chem.msu.ru/cgi-bin/tkv.pl?show=welcome.html/welcome.html.